

RESEARCH

Open Access



# Lnc-PDZD7 contributes to stemness properties and chemosensitivity in hepatocellular carcinoma through EZH2-mediated ATOH8 transcriptional repression

Yi Zhang<sup>1,2†</sup>, Bo Tang<sup>1\*†</sup>, Jun Song<sup>2</sup>, Shuiping Yu<sup>1</sup>, Yang Li<sup>1</sup>, Huizhao Su<sup>1</sup> and Songqing He<sup>1\*</sup>

## Abstract

**Background:** Hepatocellular carcinoma (HCC) with stemness features are pivotal for tumorigenesis, chemoresistance, and progression. Long non-coding RNAs have been implicated in the regulation of HCC stemness features; however, their mechanisms remain largely unknown. Here, we found that Lnc-PDZD7 is a potential oncogene. We systematically analyzed the clinical significance and mechanism of Lnc-PDZD7 in stemness and chemosensitivity regulation.

**Methods:** We analyzed the Lnc-PDZD7 expression levels in liver cancer tissues and cell line by qRT-PCR and In situ hybridization. Gain- and loss-of-function experiments were conducted to investigate the biological functions of Lnc-PDZD7 in stemness and chemosensitivity regulation. Bioinformatics analysis, dual-luciferase reporter assays were performed to validate that Lnc-PDZD7 competitively regulates EZH2. Moreover, chromatin immunoprecipitation assays, bisulfite genomic sequencing and Western blot were performed to evaluate the mechanisms of EZH2 repressing ATOH8.

**Results:** Lnc-PDZD7 is frequently upregulated in HCC tissues. Patients with high Lnc-PDZD7 expression had poorer prognoses and a poor response to adjuvant TACE therapy. Lnc-PDZD7 could promote stemness features and suppress the sensitivity of HCC cells to anticancer drugs in vitro and in vivo. Mechanistically, Lnc-PDZD7 functioned as a molecular sponge for miR-101, antagonizing its ability to repress EZH2 expression. Subsequently, EZH2 can further inhibit the expression of the stemness regulator ATOH8 via elevating its H3K27 trimethylation and DNA methylation.

**Conclusion:** Lnc-PDZD7 promotes stemness properties and suppresses chemosensitivity through the miR-101/EZH2/ATOH8 pathway, providing new biomarkers for diagnosis and potential drug targets for HCC.

**Keywords:** Hepatocellular carcinoma, Long non-coding RNAs, Lnc-PDZD7, Stemness property, Chemosensitivity

## Background

Hepatocellular carcinoma (HCC) is the sixth most common malignancy in the world with an extremely poor prognosis [1]. Although hepatic resection is a well-accepted therapy for HCC, the curative effect is not ideal. Many patients develop tumor recurrence, coupled with an inherent high

resistance to chemotherapeutic drugs. Therefore, comprehensive elucidation of the mechanisms governing rapid relapse and resistance to treatment in HCC is urgently needed.

Studies suggest that tumor cells with stemness features have strong self-renewal capacity and can be labeled by stemness-related genes, such as CD133, OCT4, NANOG and SOX2, which are pivotal for tumorigenesis, chemoresistance, and progression of HCC [2, 3]. Tumors that harbor an abundant population of tumor cells with stemness features and/or that have high expression of

\* Correspondence: [dr\\_sntangbo@163.com](mailto:dr_sntangbo@163.com); [Dr\\_hesongqing@163.com](mailto:Dr_hesongqing@163.com)

†Yi Zhang and Bo Tang contributed equally to this work.

<sup>1</sup>Department of Hepatobiliary Surgery, The First Affiliated Hospital of Guangxi Medical University, No.6 Shuangyong Road, Nanning, Guangxi 530021, People's Republic of China

Full list of author information is available at the end of the article



stemness-related genes may signal a poor outcome for HCC patients, suggesting that suppressing cancer stemness could provide a promising way to improve HCC treatment.

Long non-coding RNAs (lncRNAs) are non-coding RNAs more than 200 bp in length with no or weak protein coding abilities [4]. The molecular functions of lncRNAs include acting as host genes for microRNAs (miRNAs), preventing RNA and proteins from binding to intended targets, or serving as molecular scaffolds to guide proteins to their direct chromosomal targets [5]. Studies have reported that lncRNAs regulate various biological processes, including cell differentiation, immune response, apoptosis and especially cancer stemness [5]. Recent studies [3] showed that DANCR increases cancer stem cell (CSC) function by upregulating AXL via competitively binding to miR-33a-5p in osteosarcoma. Moreover, HOTTIP mediated HOXA9 to enhance the Wnt/ $\beta$ -catenin pathway, which is critical for the maintenance of stemness properties in human pancreatic cancer [6]. These findings suggested that lncRNAs may be stemness regulators.

In this study, we identified differential lncRNAs between 18 HCC tissues and 18 corresponding non-tumor tissues. Among them, Lnc-PDZD7 was significantly upregulated in HCC tissues. Moreover, Lnc-PDZD7 could promote stemness features and enhanced the chemoresistance of anticancer drugs in HCC cells. Interestingly, Lnc-PDZD7 increased EZH2, a histone methyltransferase, via binding to miR-101 and suppressed stemness regulator ATOH8 via controlling DNA methylation of its promoter and H3K27 methylation in HCC cells.

## Materials and methods

### Patient samples

The study was reviewed and approved by the ethics committee of The Affiliated Hospital of Guangxi Medical University, and written informed consent was obtained from all of the patients. The study included 152 patients with HCC aged 25 to 74 years; all of the patients underwent curative surgery from 2008 to 2010 at the Department of Hepatobiliary Surgery, The Affiliated Hospital of Guangxi Medical University. No patients underwent palliative resection, preoperative chemotherapy, or radiotherapy. Clinicopathological features examined included age, gender, etiology, presence of liver cirrhosis, AFP, tumor size, tumor differentiation, vascular invasion, and tumor stage. Tumors were classified and graded based on the pTNM classification advocated by the International Union Against Cancer. All 152 patients were followed for 5 years with computed tomography and ultrasonography every six months after discharge. When tumor recurrence or metastasis was suspected, therapeutic TACE was performed in 70 patients according to the tumor size and number.

### In situ hybridization (ISH)

ISH analysis was performed according to a previously described method [7]. Antisense oligonucleotide probes for Lnc-PDZD7 (Exiqon Inc. Shanghai, China) were used for ISH.

### Cell lines and cell culture

The HCC cell lines used in this study were purchased from American Type Culture Collection. These cell lines include Bel-7402, HepG2, SK-Hep-1, SNU-387 and MHCC-97H cells. All cancer cells were maintained in high-glucose Dulbecco's modified Eagle medium (DMEM; Thermo Scientific) supplemented with 10% fetal bovine serum (FBS, Gibco), 0.1 mmol/L MEM nonessential amino acids (NEAA; Invitrogen), and 1% L-glutamine (Invitrogen). All of the cell lines were cultured in 5% CO<sub>2</sub> at 37 °C in incubators at 100% humidity.

### Cell transfection

A lentiviral pGLV2-U6-Puro vector containing Lnc-PDZD7 shRNA and a negative control lentivirus were purchased from GenePharma (GenePharma, Shanghai, China). The sequence of the Lnc-PDZD7 shRNA was 5'-CCGGGCATCCAGGTAGGCACAAAGACTCG AGTCTTTGTGCCTACCTGGATGCTTTTG-3'. The lentivirus Lnc-PDZD7 shRNA or negative control was co-transfected into 293 T cells using EndoFectin Lenti transfection reagent according to the manufacturer's instructions. After culturing for 48 h, the lentiviral particles in the supernatant were harvested, filtered, and then used to transfect HepG2 cells. To select stably transduced cells, the cells were resuspended and cultured in the presence of puromycin (2  $\mu$ g/ml) for 2 weeks; qRT-PCR was performed to determine the level of Lnc-PDZD7 expression.

Short interfering RNA (siRNA) sequences were directly synthesized (GenePharma, Shanghai, China). The sequences of siRNA are as follows: Lnc-PDZD7 siRNA: UUACUCACAACUAUCCGCCAG, EZH2 siRNA: UUCA AUGAAAGUACCAUCCUG, ATOH8 siRNA: UUGG AGAAGACCACGAGGCUG. A scrambled sequence was used as a negative control of siRNA (siRNA-scr). Cells were transiently transfected with siRNA or siRNA-scr using Lipofectamine 3000 (Life technologies, Shanghai, China). Two days later, the cells were harvested for further experiments.

For gene overexpression, full length human Lnc-PDZD7, EZH2 and ATOH8 were cloned into of the pcDNA3.1 vector (Invitrogen, Shanghai, China). miR-101 mimics and inhibitor (RiboBio, Guangzhou, China) were used to overexpress or knockdown miR-101. Empty vector was used as a control. The vectors were transfected into cells using Lipofectamine 3000 (Invitrogen, Shanghai, China). Two days later, the cells were harvested for further experiments.

### Spheroid formation assay

A total of 500 single HCC cells were plated onto 24-well poly-HEMA-coated plates (Sigma-Aldrich, Shanghai, China). The cells were cultured for 3–4 weeks in DMEM/F12 medium (Invitrogen, Shanghai, China) supplemented with 4 mg/mL insulin (Sigma-Aldrich, Shanghai, China), B27 (1:50, GIBCO, Shanghai, China), 20 ng/mL EGF (Sigma-Aldrich, Shanghai, China) and 20 ng/mL basic FGF (Sigma-Aldrich, Shanghai, China). For serial passage of primary spheres, the primary spheres were collected, subsequently dissociated with trypsin and resuspended in DMEM/F12 medium with the above supplements. The surviving colonies were measured depending on their diameter, and the data are expressed as the mean  $\pm$  SD of triplicate wells within the same experiment.

### In vivo tumor growth assay

Six-week-old male BALB/c nude mice were obtained (Shanghai Slac Laboratory Animal Co. Ltd., China) and bred under specific pathogen-free conditions. Lnc-PDZD7 silenced cancer cells or empty vector control cells were subcutaneously injected into the flank region of the mice (6 mice/group). For weekly bioluminescence imaging, the mice were injected intraperitoneally with 150 mg/kg luciferin. After 10 min, tumor burden was measured in an in vivo imaging system and quantified using the Living Image software (Xenogen). Over a period of 5 weeks, tumor formation in the mice was observed by measuring the tumor volume. Then, the tumors were excised and weighed.

### DNA methylation analysis

DNA was isolated using the proteinase K/phenol extraction method. Bisulfite conversion was performed with 1  $\mu$ g of DNA using an Epiect Bisulfite Kit (Qiagen, Shanghai, China). Bisulfite-treated DNA was amplified with bisulfite-sequencing PCR (BSP) primers located in the ATOH8 promoter, forward: 5'-GAAATTGTTGTTTT TAAGAGTGATTGATA-3' and reverse: 5'-CAACCTCCC AAATAACTAAACTACA-3'. PCR products were cloned using the pGEM-T Easy Vector system (Promega, Beijing, China). Three individual clones were sequenced. The region assessed by BSP included 22 CpG sites from the ATOH8 promoter and the average methylation from individual clones was calculated as a percentage of the number of methylated CpG sites over the number of total CpG sites sequenced.

### Luciferase assay

The complementary DNA fragment containing the wild type or mutant Lnc-PDZD7 fragment and 3' untranslated region (UTR) of EZH2 was sub-cloned downstream of the luciferase gene in the pGL3-Basic

luciferase reporter vector (Promega, Beijing, China). Human liver cancer cells ( $1.0 \times 10^5$ ) grown in a 24-well plate were co-transfected with 150 ng of either the empty vector or miR-101, 50 ng of a firefly luciferase reporter comprising wild type or mutant Lnc-PDZD7 and the 3' UTR of an EZH2 fragment using Lipofectamine 3000 (Invitrogen, Shanghai, China). Forty-eight hours after transfection, the luciferase activity was determined using the Dual-Luciferase Kit (Promega, Beijing, China). The relative firefly luciferase activities were normalized to those of Renilla luciferase. Transfection was repeated in triplicate.

### Chromatin immunoprecipitation (ChIP) assay

A ChIP assay was performed using the EZ-ChIP chromatin immunoprecipitation kit (Millipore, Beijing, China). Following the manufacturer's protocol, immunoprecipitate (IP) complexes were immunoprecipitated with an anti-EZH2 and anti-H3K27me3 antibodies or a rabbit IgG antibody overnight at 4 °C. The isolated genomic DNA was obtained and used for quantitative PCR analysis. Ten percent of total genomic DNA from the nuclear extract was used as input. The primers used to detect the ATOH8 promoter sequence were as follows: forward: 5'-GCGTGACTTTGGAGCTTTCG-3' and reverse: 5'-ACTCGCCACGAGACAGAAAA-3'. The amplification efficiency was calculated, and the data were expressed as enrichment related to input.

### Biotin pull-down assay

All processes were performed in RNase-free conditions. For the antisense oligomer affinity pull-down assay, sense or antisense biotin-labeled DNA oligomers corresponding to Lnc-PDZD7 (1 mM) were incubated with lysates from HCC cells. One hour after incubation, streptavidin-coupled agarose beads (Invitrogen, Shanghai, China) were added to isolate the RNA-protein complex or RNA-RNA complex. For the in vitro RNA pull-down assay, 5 mg in vitro-synthesized biotin-labeled DNA was incubated with lysates for 3 h. Streptavidin-coupled agarose beads (Invitrogen, Shanghai, China) were then added to the reaction mix to isolate the RNA-protein complex or RNA-RNA complex. Immunocomplexes were then analyzed by real-time RT-PCR or Western blotting.

### Quantitative real time RT-PCR (qRT-PCR)

Total RNA was extracted from cells or tissues using TRIzol (Invitrogen, Shanghai, China) according to the manufacturer's protocol. cDNA synthesis was performed using the PrimeScript RT reagent Kit (TaKaRa, Dalian, China). Real-time qRT-PCR analysis was performed using Platinum SYBR Green qPCR SuperMix-UDG kits (Life Technologies, Gaithersburg, MD, USA) or a

TaqMan Probe Master Mix kit (Vazyme Biotech Co., Nanjing, China) according to the manufacturer's protocol. The expression of EZH2, ATOH8, CD133, OCT4, NANOG, SOX2 and Lnc-PDZD7 were equilibrated to  $\beta$ -actin. miR-101 was normalized to U6. The primers used for amplification were as follows:

Lnc-PDZD7: forward 5'-AGAGCCCGCGGATT TTA AAC-3'.

reverse 5'-GTGATTCCATTCGTCAGCCC-3'

miR-101: forward 5'-TAAGGCACCCTTCTGAGTGA-3'

reverse 5'-GCGAGCACAGAATTAATACGAC-3'

EZH2: forward (5'-GCCAGACTGGGAAGAAATCTG-3')

reverse (5'-TGTGCTGGAAAATCCAAGTCA-3')

ATOH8: forward (5'-CAGGTGCCGTGCTACTCAT A-3')

reverse (5'-AGTCACTCCTTGCGCTTCTT-3')

CD133: forward (5'-TGGATGCAGAACTTGACAA CGT-3')

reverse (5'-ATACCTGCTACGACAGTCGTGGT-3')

OCT4: forward (5'-CGACCATCTGCCGCTTTGAG-3')

reverse (5'-CCCCCTGTCCCCATTCCTA-3')

NANOG: forward (5'-AAGGTCCCGGTCAAGAAAC AG-3')

reverse (5'-CTTCTGCGTCACACCATTGC-3')

SOX2: forward (5'-TGGACAGTTACGCGCACAT-3')

reverse (5'-CGAGTAGGACATGCTGTAGGT-3')

$\beta$ -actin: forward (5'-CATGTACGTTGCTATCCAG GC-3')

reverse (5'-CTCCTTAATGTCACGCACGAT-3')

U6: forward (5'-AAAGCAAATCATCGGACGACC-3')

reverse (5'-GTACAACACATTGTTTCTCGGA-3')

#### MTT assay

Cells were transfected as indicated previously and treated with or without different concentrations of 5-Fu or sorafenib. Cells were seeded on a 96-well plate at a density of  $1 \times 10^3$  cells/well. After incubation for 48 h at 37 °C in a humidified incubator, 20  $\mu$ l of MTT (5 mg/ml in PBS) was added to each well, and the cells were incubated for a further 4 h. After removal of the medium, 150  $\mu$ l of DMSO was added to each well. The absorbance at a wavelength of 540 nm was recorded using a microplate reader.

#### Western blot analysis

Tissues or cells were homogenized and lysed with lysis buffer (50 mM Tris-HCl, 137 mM NaCl, 10% glycerol, 100 mM sodium orthovanadate, 1 mM phenylmethylsulfonyl fluoride (PMSF), 10 mg/ml aprotinin, 10 mg/ml leupeptin, 1% Nonidet P-40, and 5 mM protease inhibitor

cocktail; pH 7.4). After protein concentration determination using a BCA assay,  $\beta$ -mercaptoethanol and bromophenol blue were added to the sample buffer for electrophoresis. The proteins were separated via 10% PAGE and transferred to polyvinylidene difluoride membranes (Bio-Rad, Shanghai, China). The membranes were incubated in a primary antibody overnight at 4 °C. After incubation with a secondary antibody for 2 h, the reactive bands were visualized using an enhanced chemiluminescence system. The intensities of the bands were quantified using an image analysis system.

#### Immunohistochemistry (IHC)

The tissue sections were deparaffinized in xylene and rehydrated using a graded ethanol series. To quench endogenous peroxidase activity, the sections were immersed in a 0.3% peroxidase-methanol solution for 30 min. For antigen retrieval, the sections were pretreated with citrate buffer for 15 min at 100 °C in a microwave oven. The sections were hybridized with a primary antibody against EZH2 and ATOH8 (Santa Cruz, Texas, USA) at 4 °C overnight at a dilution of 1:100 and were visualized using the UltraVision Quanto Detection System HRP DAB kit (Thermo Scientific, Shanghai, China) according to the manufacturer's protocols. The stained sections were counterstained with hematoxylin, and photomicrographs were captured using an Olympus BX51 microscope.

#### Northern blotting

Total RNA was extracted from HCC cells using standard TRIZOL methods, followed by electrophoresis with formaldehyde denaturing agarose gel. Samples were transferred to positively charged NC film. After ultraviolet cross-linking, the membrane was incubated with hybrid buffer for a 2-h prehybridization, followed by incubation with biotin-labeled RNA probes. Biotin signals were detected with HRP-conjugated streptavidin according to the instructions of the Chemiluminescent Nucleic Acid Detection Module (Thermo Scientific, Shanghai, China).

#### Microarray analysis

We identified differential LncRNAs between 18 HCC tissues and 18 corresponding non-tumor tissues. Total RNA was extracted using TRIzol Reagent (Invitrogen, CA, USA) according to the manufacturer's protocol. RNA quantity was measured by the NanoDrop ND-2000 spectrophotometer (OD 260 nm, NanoDrop, Wilmington, DE, USA), and RNA integrity was assessed using standard denaturing agarose gel electrophoresis. Microarray analysis LncRNA expression profiling was performed by an Arraystar Human LncRNA Microarray V3.0 platform (Agilent Technologies, Beijing, China).

Differentially expressed lncRNAs were identified by  $P$  value/false discovery rate filtering.

### Statistical analysis

All values are expressed as the means  $\pm$  standard deviation (SD). The significance of the differences was determined via one-way ANOVA or Student's  $t$ -test. The Chi-squared test was used to evaluate the relationship between expression and the clinicopathological characteristics. Spearman's correlation coefficient was used to calculate the correlations between two groups. Kaplan-Meier analysis was employed for survival analysis, and the differences in the survival probabilities were estimated using the log-rank test.  $P < 0.05$  was considered significant. Statistical analysis was performed using SPSS version 17.0 (SPSS, Inc.).

### Results

#### Lnc-PDZD7 is identified as an upregulated lncRNA and is associated with poor response to adjuvant TACE in HCC

We employed a lncRNA microarray analysis of 18 HCC tissues and corresponding para-tumorous tissues to identify lncRNAs that are dysregulated in HCC. We

found that 26 lncRNAs were significantly upregulated in HCC tissues compared to para-tumorous tissues ( $P < 0.01$  and fold change  $> 6$ , Additional file 1: Figure S1). Among them, we are interested in Lnc-PDZD7 (ENST00000609242.1).

We analyzed Lnc-PDZD7 expression levels in liver tissues, and qRT-PCR revealed that Lnc-PDZD7 expression was higher in HCC cases compared with peritumorous tissues (Fig. 1a). ISH further confirmed that Lnc-PDZD7 was mainly located in the cytoplasm (Fig. 1b). Then, we examined the correlation of Lnc-PDZD7 expression with clinicopathological findings in 152 HCC cases. The patients were stratified into 2 groups based on the median Lnc-PDZD7 expression levels detected by qRT-PCR. The Lnc-PDZD7 levels were significantly associated with tumor stage, tumor size, tumor differentiation, vascular invasion and TACE treatment (Table 1). We examined the correlation between Lnc-PDZD7 expression and five-year follow-up of the patients. Using the middle expression value of Lnc-PDZD7 in 152 cases of patients as the cut-off point, Kaplan-Meier analysis revealed that the patients with high expression of Lnc-PDZD7 had a significantly lower overall survival

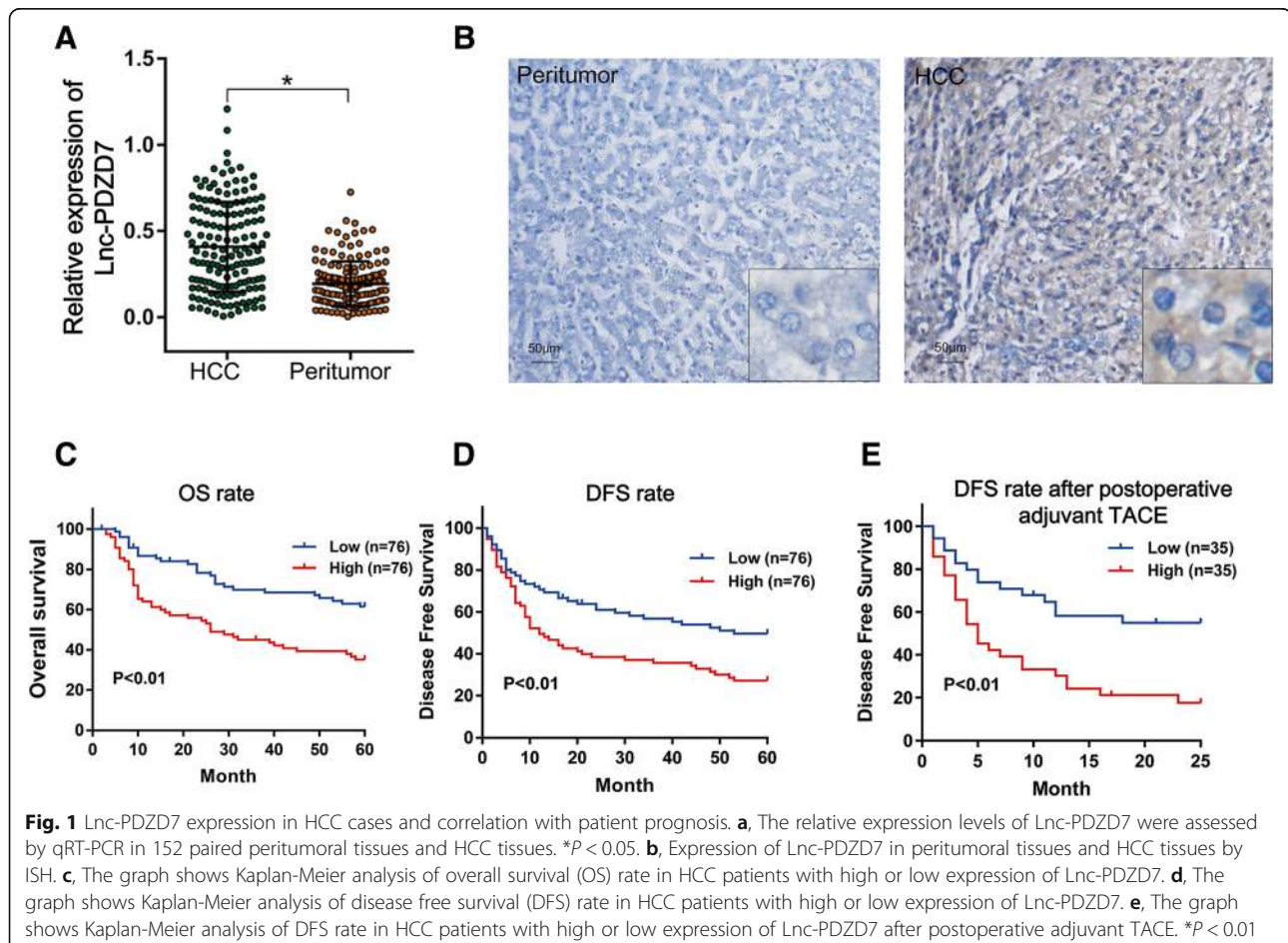




**Table 1** Relationship between Lnc-PDZD7 and clinicopathological parameters in 152 HCC patients

Variables	Number of cases	Lnc-PDZD7 expression		P value
		Low N = 76	High N = 76	
Age (years)				
≥ 50	25	14	11	0.512
< 50	127	62	65	
Gender				
Male	101	45	56	0.059
Female	51	31	20	
Tumor number				
Single	127	67	60	0.126
Multiple	25	9	16	
Etiology				
viral	119	58	61	0.555
Non-viral	33	18	15	
Serum AFP (ng/ml)				
≤ 200	84	37	47	0.103
> 200	68	39	29	
Tumor stage				
I/II	87	54	33	0.001
III/IV	65	22	43	
Tumor size (cm)				
≤ 5	67	40	27	0.034
> 5	85	36	49	
Tumor differentiation				
Well	61	37	24	0.001
Moderate	45	21	24	
Poor	46	17	29	
Vascular invasion				
Yes	46	17	29	0.034
No	106	59	47	
TACE treatment				
Yes	70	28	41	0.023
No	82	48	35	

(OS) rate than the patients with low expression of Lnc-PDZD7 (OS rate: 35.1% versus 61.5%) (Fig. 1c). Furthermore, the patients with low expression of Lnc-PDZD7 had a higher disease free survival (DFS) rate (DFS rate: 27.1% versus 49.7%) (Fig. 1d). Then, we further examined whether Lnc-PDZD7 is an independent prognostic factor based on multivariate Cox analysis. We found that the following factors were significantly related to OS and DFS: tumor stage, tumor size, tumor differentiation and Lnc-PDZD7 expression level (Additional file 2: Table S1). Our results indicated that Lnc-PDZD7 is not an independent prognostic factor.

Adjuvant TACE is one of the most used methods to prevent tumor recurrence. Next, we evaluated DFS rate after postoperative adjuvant TACE, which was associated with the response to adjuvant TACE therapy. TACE treatment was significantly correlated with Lnc-PDZD7 expression (Table 1). Kaplan-Meier analysis revealed that the patients with high expression of Lnc-PDZD7 had a higher DFS rate than patients with low expression of Lnc-PDZD7 (Fig. 1e), indicating that the patients with high expression of Lnc-PDZD7 had a poor response to adjuvant TACE therapy.

#### Lnc-PDZD7 suppresses the stemness property and enhances the chemosensitivity of HCC cells

We examined the Lnc-PDZD7 expression level in HCC cell lines, Bel-7402, HepG2, SK-Hep-1, SNU-387 and MHCC-97H, by qRT-PCR. Among HCC cells, HepG2 and Bel-7402 showed relatively higher and lower expression of Lnc-PDZD7 (Fig. 2a). Northern blotting with the total RNA of HepG2 and Bel-7402 cells confirmed that the length of transcripts is approximately 970 nt (Fig. 2b). ISH was conducted to analyze the location, and we found that Lnc-PDZD7 is mainly localized in the cytoplasm (Fig. 2c).

As Lnc-PDZD7 level could predict the response to TACE, we wanted to investigate the effect of Lnc-PDZD7 on stemness features and the chemosensitivity of HCC cells. In HepG2 cells, ectopic suppression of Lnc-PDZD7 reduced spheroid formation ability compared with control (Fig. 2d). Conversely, Lnc-PDZD7 overexpression enhanced the spheroid formation ability in Bel-7402 cells (Fig. 2e). We examined the potential regulatory effect of Lnc-PDZD7 on the expression of CSC marker CD133 and stemness-associated genes, including OCT4, NANOG, and SOX2. Suppression of Lnc-PDZD7 significantly reduced the expression of CD133, OCT4, NANOG, and SOX2 in HepG2 cells (Fig. 2f and Additional file 3: Figure S2). Moreover, Lnc-PDZD7 overexpression significantly increased the expression of CD133, OCT4, NANOG, and SOX2 in Bel-7402 cells (Fig. 2g and Additional file 3: Figure S2). Thus, overexpression of Lnc-PDZD7 may promote the stemness feature of HCC cells.

Next, we wanted to determine whether Lnc-PDZD7 can affect chemosensitivity to 5-fluorouracil (5-Fu) and sorafenib in HCC cells. Sorafenib is in a class of medications called kinase inhibitors and is used to treat advanced renal cell carcinoma and HCC. Ectopic suppression of Lnc-PDZD7 sensitized HepG2 cells to 5-Fu as reflected by reduced cell viability (Fig. 3a), colony formation (Fig. 3b), and in vivo tumorigenicity (Fig. 3c, d). Overexpression of Lnc-PDZD7 by the Lnc-PDZD7 plasmid reduced the sensitivity of Bel-7402 cells to sorafenib as reflected by increased cell viability (Fig. 3e), colony formation (Fig. 3f), and in vivo tumorigenicity (Fig. 3g, h).

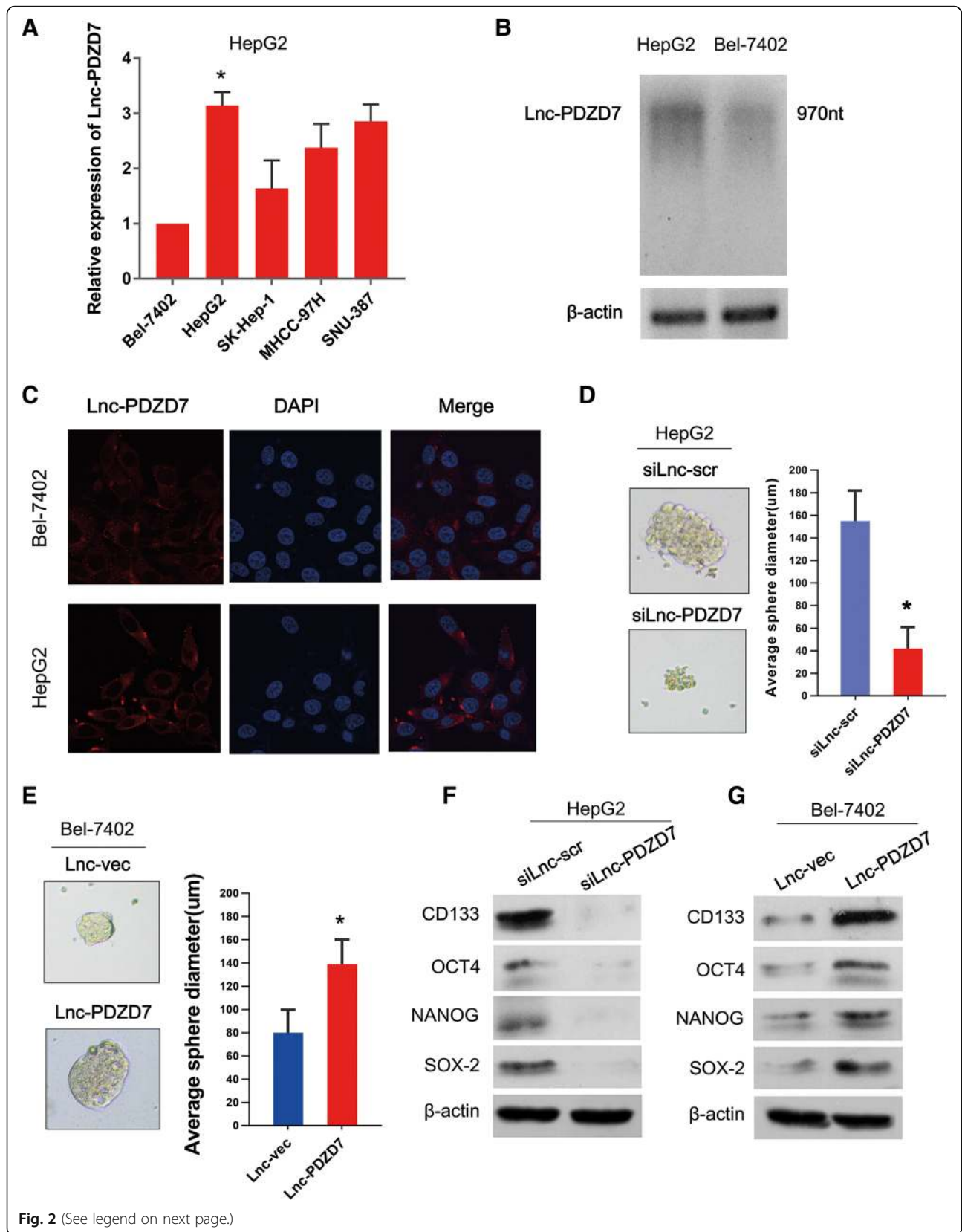


Fig. 2 (See legend on next page.)

(See figure on previous page.)

**Fig. 2** Lnc-PDZD7 suppresses the stemness of HCC cells. **a**, Expression of Lnc-PDZD7 was examined in Bel-7402, HepG2, SK-Hep-1, SNU-387 and SMMC-7721 cell lines by qRT-PCR. The data are shown as the means  $\pm$  S.D. \*Compared to Lnc-PDZD7 expression in LO2 ( $P < 0.05$ ). **b**, Total RNA from the indicated cell lines was subjected to northern blot analysis to determine the molecular size and the expression level of Lnc-PDZD7. **c**, FISH was used to detect the endogenous Lnc-PDZD7 molecules (red) in Bel-7402 and HepG2. **d-e**, Representative images of sphere formation induced by sh-Lnc-PDZD7 or over-Lnc-PDZD7 transfection in HepG2 or Bel-7402, respectively. The surviving colonies were measured depending on their diameter. The data are shown as the mean  $\pm$  SD of triplicate wells within the same experiment. \* $P < 0.05$ . **f-g**, Expression of CD133 and stemness-associated genes, including OCT4, NANOG and SOX2, was examined in siLnc-PDZD7 transfected HepG2 cells and over-Lnc-PDZD7 transfected Bel-7402 cells by Western blot. The data are shown as the means  $\pm$  S.D. \* $P < 0.05$

### Lnc-PDZD7 upregulates EZH2 by competitively binding miR-101 in HCC

In order to explore the mechanism regarding Lnc-PDZD7 regulating the stemness property and chemosensitivity, all the mRNAs of HepG2 cells before and after Lnc-PDZD7 knockdown were selected for comparison. Among differentially expressed mRNA, EZH2 mRNA level was significantly decreased (Fig. 4a). It is reported that EZH2 has a critical function in maintaining stemness properties in solid tumors, like glioblastoma and breast cancer [8–10]. However, the EZH2 regulation mechanism of the hepatic cancer stemness is not well understood. We hypothesized that Lnc-PDZD7 may function through EZH2. To test this hypothesis, we examined Lnc-PDZD7 and EZH2 expression in 152 HCC tissues by qRT-PCR, demonstrating that Lnc-PDZD7 was positively correlated with EZH2 expression ( $r = 0.628$ , Fig. 7b). In addition, Lnc-PDZD7 knockdown in HepG2 cells downregulated EZH2 while Lnc-PDZD7 overexpression upregulated EZH2 in Bel-7402 cells (Fig. 4b), suggesting that Lnc-PDZD7 can promote EZH2 expression in HCC.

LncRNAs in the cytoplasm have been postulated to act as a competing endogenous RNA, interacting with microRNAs in a manner that can sequester these molecules and reduce their regulatory effect on target mRNA [11]. Next, we investigated whether miRNAs are involved in Lnc-PDZD7 promoting EZH2. Some studies showed that EZH2 has been proposed to be a target gene of miR-101 in HCC [12, 13]. Moreover, target prediction algorithms predicted that miR-101 has binding sites for Lnc-PDZD7. Therefore, we speculated that Lnc-PDZD7 can regulate EZH2 expression via miR-101. We overexpressed Lnc-PDZD7 in HepG2 cells and found that the levels of miR-101 decreased significantly, whereas Lnc-PDZD7 knockdown displayed an opposite effect (Fig. 4c). To examine the potential lncRNA-miRNA interaction, we subcloned full-length Lnc-PDZD7 or Lnc-PDZD7 harboring a site-directed mutation in the miR-101-binding site into the luciferase reporter vector (referred to as Lnc-PDZD7-wt or Lnc-PDZD7-mut, respectively; Fig. 4d). The miR-101-mediated suppression of luciferase activity

was abolished in this mutated Lnc-PDZD7 construct compared with the wild-type vector (Fig. 4e). Meanwhile, a Lnc-PDZD7 specific probe was used to perform RNA precipitation, and the results demonstrated a specific enrichment of miR-101 in the precipitates of Lnc-PDZD7 (Additional file 4: Figure S3A). Subsequently, we performed a luciferase reporter assay to verify the interaction between miR-101 and EZH2. Consistent with previous reports, dual-luciferase assays showed that overexpression of miR-101 resulted in a significant decrease in the luciferase activity of EZH2 wt but not EZH2 mut (Additional file 4: Figure S3B and C).

### Upregulation/downregulation of EZH2 partially rescues Lnc-PDZD7-mediated stemness and chemoresistant properties in HCC cells

To further confirm the roles of EZH2 in Lnc-PDZD7-mediated stemness and chemoresistant properties, we constructed a plasmid containing full length EZH2 (EZH2wt) and a control empty vector (vector). EZH2wt or vector was transfected into HepG2 cells with Lnc-PDZD7 knocked down. In Lnc-PDZD7-downregulated HepG2 cells, EZH2wt, but not vector, rescued the decreased expression of CSC biomarkers (Fig. 4f and Additional file 5: Figure S4A) and suppressed spheroid formation (Additional file 5: Figure S4B). Furthermore, EZH2wt enhanced the decreased cell viability of Lnc-PDZD7-knockout HepG2 cells after treatment with 5-Fu (Additional file 5: Figure S4C).

Then, we generated EZH2 siRNA (siEZH2) and its scramble control (siEZH2scr). siEZH2, but not siEZH2scr, reduced the protein and mRNA expression of EZH2 in Lnc-PDZD7 overexpressed Bel-7402 cells (Fig. 4g and Additional file 5: Figure S4D). Consistent with the above results, siEZH2, but not siEZH2scr, decreased the upregulated expression of CSC biomarkers (Fig. 4g and Additional file 5: Figure S4D) and spheroid formation (Additional file 5: Fig. S4E). In addition, EZH2 siRNA significantly reduced the cell viability by sorafenib treatment in Lnc-PDZD7 overexpressed Bel-7402 cells (Additional file 5: Figure S4F). These findings suggest that EZH2 may be involved in Lnc-PDZD7-mediated stemness and chemoresistant properties in HCC cells.



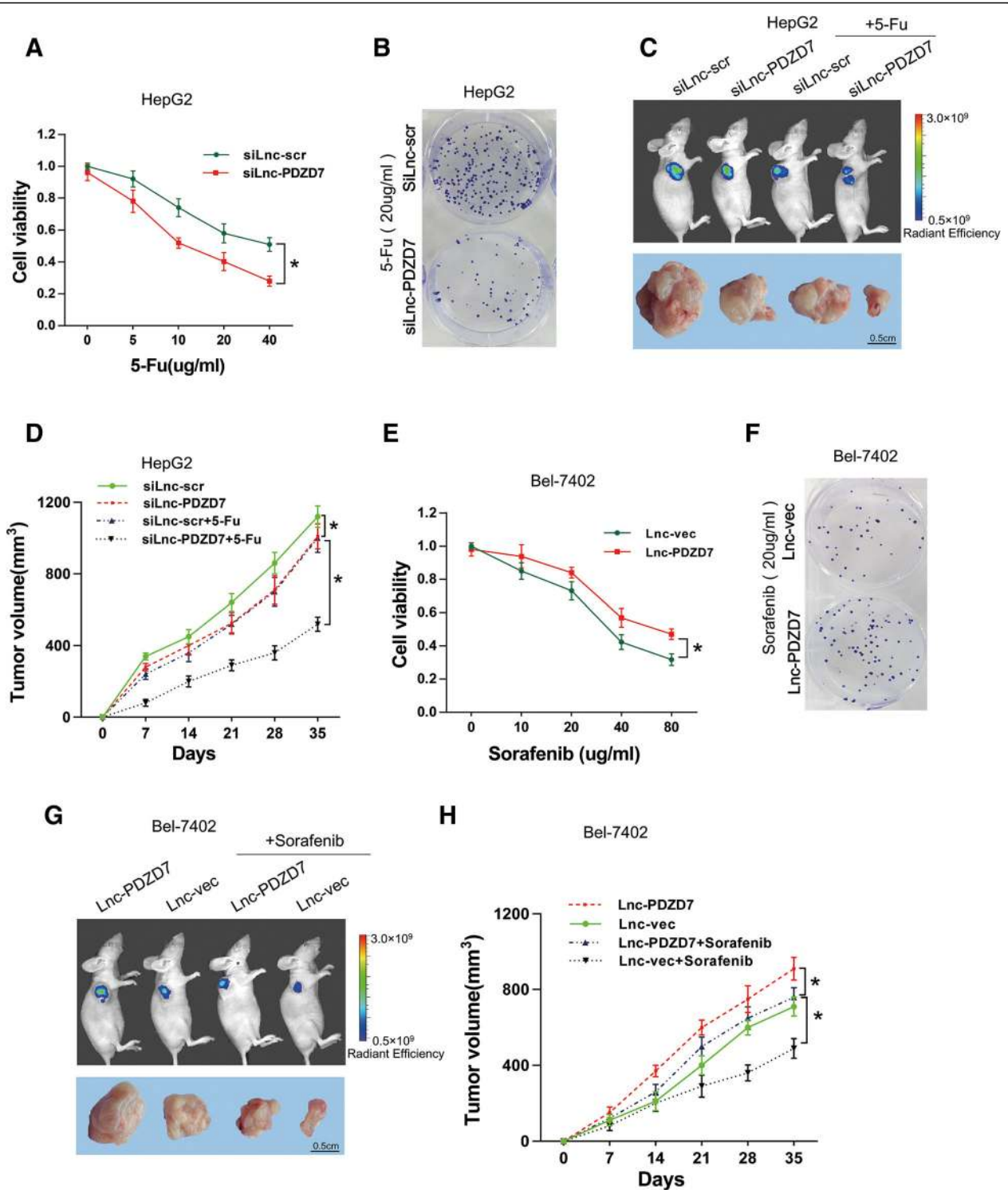


Fig. 3 (See legend on next page.)

(See figure on previous page.)

**Fig. 3** Lnc-PDZD7 suppresses the chemoresistance of HCC cells. **a**, Cell viability was examined by MTT assay. The left graph shows the cell viability under different concentrations of 5-Fu treatment in siLnc-PDZD7 or siLnc-scr transfected HepG2 cells. **b**, A representative image of colony formation after treatment with 5-Fu in siLnc-PDZD7 or siLnc-scr transfected HepG2 cells. **c**, Tumor formation of siLnc-PDZD7 or siLnc-scr transfected HepG2 cells. Cells were injected subcutaneously into the flanks of nude mice. Then, the mice were injected intraperitoneally with 5-Fu. After four weeks, the tumors in the mice were examined by bioluminescence imaging. Representative images of tumors in each experimental group are shown. **d**, The tumor growth curves of each group of mice are shown. Six mice were used in each group. The data are shown as the means  $\pm$  S. D (\* $P$  < 0.05). **e**, Cell viability under different concentrations of sorafenib treatment in Lnc-PDZD7 or Lnc-vec transfected Bel-7402 cells. The data are shown as the means  $\pm$  S. D (\* $P$  < 0.05). **f**, A representative image of colony formation after treatment with sorafenib in Lnc-PDZD7 or Lnc-vec transfected Bel-7402 cells. **g**, Tumor formation of Lnc-PDZD7 or Lnc-vec transfected Bel-7402 cells in nude mice. The mice were injected intraperitoneally with sorafenib. **h**, The tumor growth curves of each group of mice are shown. Six mice were used in each group. The data are shown as the means  $\pm$  S. D (\* $P$  < 0.05)

### The Lnc-PDZD7-EZH2 axis increased stemness properties and decreased cancer chemosensitivity via suppressing ATOH8

We next sought to investigate the molecular mechanism regarding the Lnc-PDZD7-EZH2 axis-mediated stemness and chemoresistant properties in HCC cells. ATOH8 belongs to a group of basic-helix-loop-helix (bHLH) transcription factors and is a stemness regulator [14]. Song et al. showed that ATOH8 is frequently downregulated in HCC and can inhibit the stem cell features of HCC via repressing the transcription of OCT4, NANOG, and CD133 and sensitizing cells to chemotherapy [2]. These phenotypes, mediated by ATOH8, are similar to those mediated by Lnc-PDZD7-EZH2. Therefore, we examined the correlation between the Lnc-PDZD7-EZH2 axis and ATOH8. Interestingly, knocking down Lnc-PDZD7 upregulated ATOH8 expression in HepG2 cells and HepG2 spheres, and EZH2 overexpression by EZH2 plasmid inhibited the upregulation of ATOH8 induced by Lnc-PDZD7 siRNA in HepG2 cells (Fig. 5a, Additional file 6: Figure S5). In contrast, ectopic overexpression of Lnc-PDZD7 downregulated ATOH8 expression in Bel-7402 cells and Bel-7402 spheres, and EZH2 siRNA rescued the downregulation of ATOH8 by Lnc-PDZD7 overexpression in Bel-7402 cells (Fig. 5h, Additional file 6: Figure S5).

We examined the roles of ATOH8 in the Lnc-PDZD7-EZH2 axis-mediated stemness and chemoresistant properties in HCC cells. ATOH8 knockdown by ATOH8 siRNA rescued the suppression of CSC biomarkers, spheroid formation, and chemoresistance to 5-Fu induced by Lnc-PDZD7 inhibition (Fig. 5b-d). Moreover, ATOH8 knockdown rescued the suppression of CSC biomarkers, spheroid formation, and chemoresistance to 5-Fu induced by EZH2 knockdown (Fig. 5e-g).

Alternatively, ectopic overexpression of ATOH8 inhibited the upregulation of CSC biomarkers, the increased spheroid formation ability, and the increased chemoresistance to sorafenib induced by Lnc-PDZD7 overexpression (Fig. 5i-k). Moreover, ectopic overexpression of ATOH8 inhibited the upregulation of CSC biomarkers, the increased spheroid formation ability, and the

increased chemoresistance to sorafenib induced by EZH2 overexpression (Fig. 5l-n). These findings suggest that Lnc-PDZD7-EZH2 activation may lead to increased stemness properties and decreased cancer chemosensitivity via inhibiting the expression of ATOH8 in HCC cells.

### EZH2 represses ATOH8 by controlling DNA methylation of its promoter and H3K27 methylation

The ATOH8 promoter is located in a typical CpG island, suggesting a possible involvement of DNA methylation in the regulation of ATOH8 transcription (Fig. 6a). We examined the methylation status of the ATOH8 promoter in HCC cell lines, Bel-7402, HepG2, SK-Hep-1, SNU-387 and MHCC-97H, by BSP (bisulfite genomic sequencing). CpG islands were heavily methylated in HCC cells, especially in HepG2 (Fig. 6b). After treating HepG2 cells with 5-aza-20-deoxycytidine (5-aza-dc) for 72 h, ATOH8 expression was significantly increased (Fig. 6c). Furthermore, ATOH8 methylation was assessed in 12 pairs of HCC and their peritumoral tissues. Peritumoral tissues showed a lower methylation level with higher expression of ATOH8 compared with HCC tissues (Fig. 6d and e). As EZH2 is known to be associated with DNA methylation, we investigated whether EZH2 knockdown can increase the expression of ATOH8 by altering the hypermethylation status in HepG2 and Bel-7402 cells. MSP (methylation-specific PCR) analysis showed that the unmethylated band increased and the methylated band decreased after EZH2 knockdown in both HepG2 and Bel-7402 cells (Fig. 6f). Indeed, the mRNA and protein level of ATOH8 was upregulated by EZH2 knockdown in HepG2 cells (Fig. 6g). EZH2 overexpression decreased ATOH8 expression in Bel-7402 cells (Fig. 6G).

Recent studies strongly suggest that basic DNA methylation profile establishment might be mediated through histone modification [15]. We further investigated whether EZH2-mediated promoter H3K27 methylation can interfere with ATOH8 expression. We examined the effect of EZH2 on the expression of trimethylated Lys27 of histone 3 (H3K27me3) in HCC cells. As expected,

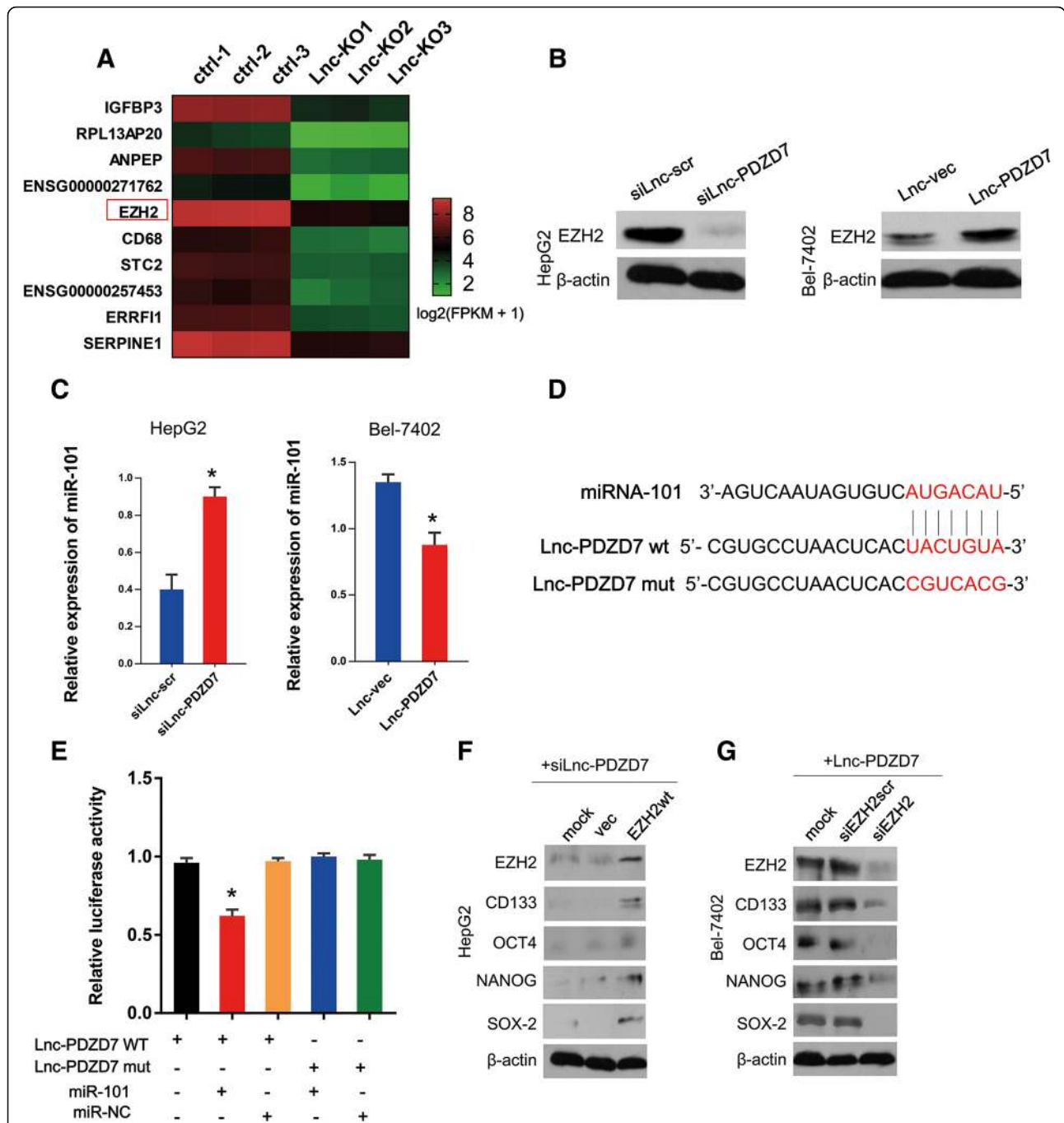


**Fig. 4** Lnc-PDZD7 upregulates EZH2 by competitively binding miR-101 in HCC. **a**, The gene expression were analyzed by the mRNA microarray in Lnc-PDZD7 down-regulated HepG2 cells. Top 10 downregulated genes were shown in the heatmap. **b**, The protein level of EZH2 was detected by Western blotting in siLnc-PDZD7 or siLnc-scr transfected HepG2 cells and Lnc-PDZD7 or Lnc-vec transfected Bel-7402 cells.  $\beta$ -Actin was used as a loading control. **c**, The expression of miR-101 was determined using qRT-PCR in cells transfected with siLnc-PDZD7 or Lnc-PDZD7. **d**, Binding sites of miR-101 in the 3'UTR of Lnc-PDZD7 (Lnc-PDZD7 wt) was predicted using bioinformatics prediction tools. The mutated site in the 3'UTR of Lnc-PDZD7 is shown as Lnc-PDZD7 mut. **e**, The relative luciferase activities were analyzed in HepG2 cells co-transfected with miR-101 mimics or miR-NC and luciferase reporter vectors psiCHECK2- Lnc-PDZD7-WT or psiCHECK2- Lnc-PDZD7-Mut. **f**, The protein expression were examined by Western blotting in EZH2 plasmid or EZH2-vec transfected Lnc-PDZD7-depleted HepG2 cells. **g**, The protein expression were examined by Western blotting in shEZH2 or shEZH2scr transfected Lnc-PDZD7-overexpressing Bel-7402 cells. The data are shown as the means  $\pm$  S.D. of three replicates (\* $P < 0.05$ )

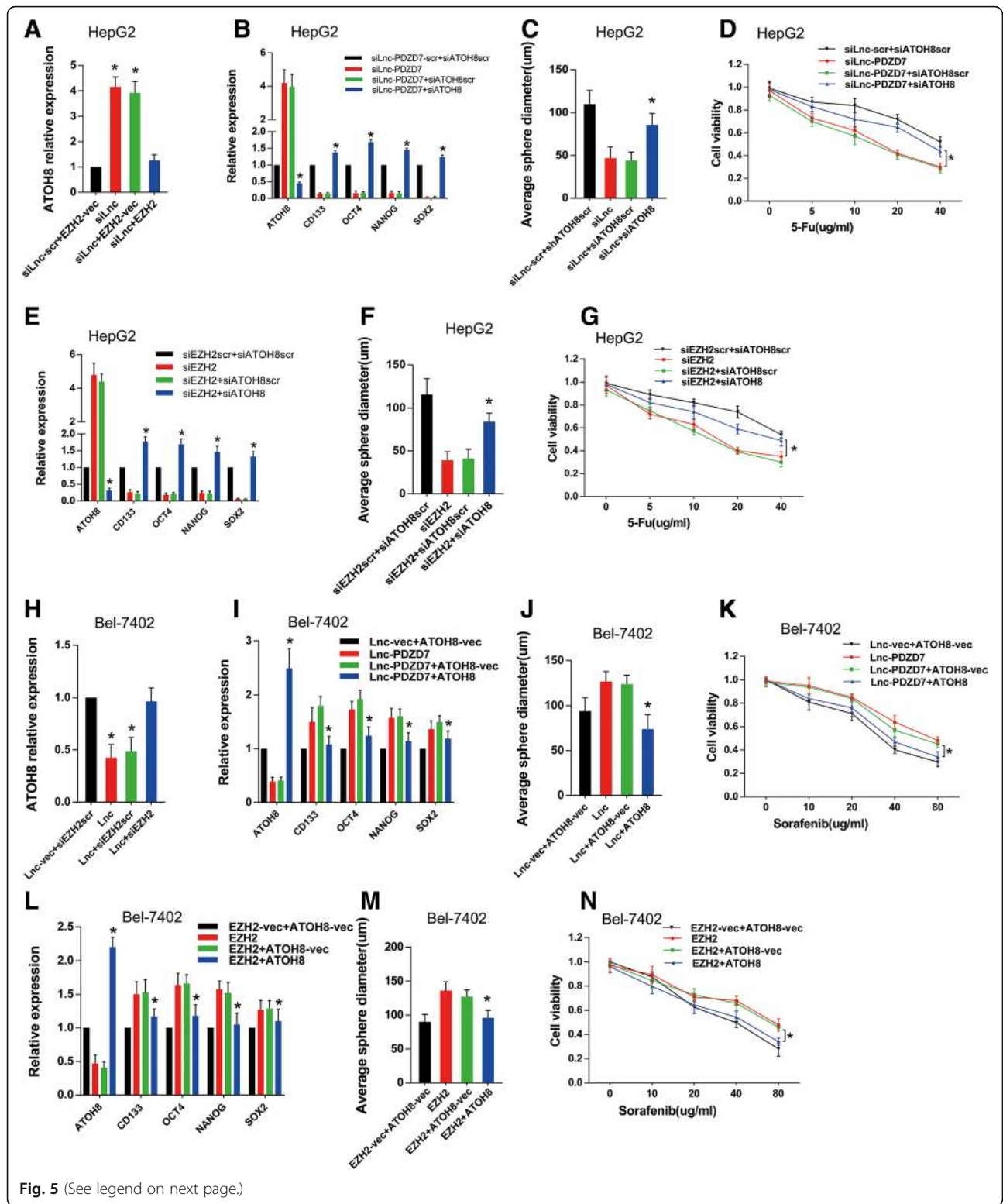


Fig. 5 (See legend on next page.)



(See figure on previous page.)

**Fig. 5** The Lnc-PDZD7-EZH2-ATOH8 axis regulates stemness properties and chemosensitivity in HCC cells. **a**, The expression of ATOH8 was examined by qRT-PCR in Lnc-PDZD7-depleted HepG2 cells with EZH2 or EZH2-vec transfection. **b**, The expression of ATOH8 and CSC markers was examined by qRT-PCR in Lnc-PDZD7-depleted HepG2 cells with shATOH8 or shATOH8scr transfection. **c**, Sphere formation in Lnc-PDZD7-depleted HepG2 cells with shATOH8 or shATOH8scr transfection and EZH2-depleted HepG2 cells with shATOH8 or shATOH8scr transfection. **d**, Cell viability under different concentrations of 5-Fu treatment in Lnc-PDZD7-depleted HepG2 cells with shATOH8 or shATOH8scr transfection. **e**, The expression of ATOH8 and CSC markers was examined by qRT-PCR in EZH2-depleted HepG2 cells with shATOH8 or shATOH8scr transfection. **f**, Sphere formation in EZH2-depleted HepG2 cells with shATOH8 or shATOH8scr transfection. **g**, Cell viability under different concentrations of 5-Fu treatment in EZH2-depleted HepG2 cells with shATOH8 or shATOH8scr transfection. **h**, The expression of ATOH8 was examined by qRT-PCR in Lnc-PDZD7-overexpressing Bel-7402 cells with shEZH2 or shEZH2scr transfection. **i**, The expression of ATOH8 and CSC markers was examined by qRT-PCR in Lnc-PDZD7-overexpressing Bel-7402 cells with or without ATOH8. **j**, Sphere formation in Lnc-PDZD7-overexpressing Bel-7402 cells with or without ATOH8. **k**, Cell viability under different concentrations of sorafenib treatment in Lnc-PDZD7-overexpressing Bel-7402 cells with or without ATOH8. **l**, The expression of ATOH8 and CSC markers was examined by qRT-PCR in EZH2-overexpressing Bel-7402 cells with or without ATOH8. **m**, Sphere formation in EZH2-overexpressing Bel-7402 cells with or without ATOH8. **n**, Cell viability under different concentrations of sorafenib treatment in EZH2-overexpressing Bel-7402 cells with or without ATOH8 ( $n = 3$ ,  $*P < 0.05$ )

EZH2 knockdown led to a decrease in H3K27me3 level with an upregulation of ATOH8 expression (Fig. 6g). Alternatively, EZH2 overexpression led to an increase in the H3K27me3 level with a downregulation of ATOH8 expression (Fig. 6g). To assess whether the promoter of ATOH8 is directly regulated by EZH2, a ChIP assay was performed in HCC cells. EZH2 was present at the proximal promoter of ATOH8 in HepG2 cells. Using an antibody specific for H3K27me3, we observed relatively high levels of H3K27me3 at the promoter of the ATOH8 gene in Bel-7402 cells (Fig. 6h and i). In contrast, EZH2 and H3K27me3 accumulated upstream of ATOH8 after EZH2 overexpression in Bel-7402 cells (Fig. 5h and i). These findings indicate a link between the epigenetic regulation and transcription of ATOH8 by EZH2 in HCC cells (Fig. 7c).

#### The clinical correlation between Lnc-PDZD7, EZH2, ATOH8 and TACE response in HCC

We further investigated the relationship of Lnc-PDZD7, EZH2, ATOH8 and TACE response in HCC cases. We examined Lnc-PDZD7 expression by ISH and expression of EZH2 and ATOH8 by IHC. As shown in Fig. 7a, patient #1 with a poor response to TACE showed higher levels of Lnc-PDZD7 and EZH2 and a lower level of ATOH8 while patient #2 with a good response to TACE showed lower levels of Lnc-PDZD7 and EZH2 and a higher level of ATOH8. Correlation analysis according to qRT-PCR results showed that the Lnc-PDZD7 level was significantly correlated with EZH2 expression in HCC tissues ( $r = 0.628$ , Fig. 7b). Lnc-PDZD7 expression was inversely correlated with ATOH8 ( $r = -0.595$ ) and EZH2 ( $r = -0.697$ ) expression in HCC tissues (Fig. 6b).

#### Discussion

Studies have confirmed that cancer stem cells have intrinsic chemoresistant properties and can be selectively enriched during chemotherapy and ultimately cause chemotherapy failure and cancer recurrence [16–18].

Therefore, enhanced stemness property of cancer imply the weakened chemosensitivity. In addition, emerging evidence has demonstrated that lncRNAs play important roles in the regulation of stemness features [3].

In our study, we identified Lnc-PDZD7 as a differentially expressed lncRNA between tumor and non-tumor tissues. Lnc-PDZD7 is an intergenic ncRNA, approximately 977 bp in length, but its function remains unknown. Our clinicopathological investigation found that Lnc-PDZD7 was associated with inferior prognosis and poor response to TACE. Therefore, we speculated that Lnc-PDZD7 participated in the regulation of stemness features and chemosensitivity of HCC. We found that Lnc-PDZD7 can enhance spheroid formation ability, increase the expression of CSC markers and reduce the chemosensitivity to 5-Fu and sorafenib in vivo and in vitro.

Next, we sought to identify the underlying molecular mechanisms by which Lnc-PDZD7 regulated downstream effectors in HCC. We performed the mRNA microarray before and after Lnc-PDZD7 knockdown, finding that EZH2 mRNA level was significantly decreased. Studies have shown that EZH2 has a critical function in maintaining stemness properties in various solid tumors, such as breast cancer and glioma [19–21]. Our results demonstrated that EZH2 plays a key role in lncRNA-mediated regulation of stemness features and chemosensitivity.

lncRNAs can sequester miRNA to regulate and communicate with mRNAs. Bioinformatics analysis indicates that Lnc-PDZD7 contains putative binding sites for miR-101. Moreover, EZH2 is one of the potential miR-101 targets in liver cancer [12]. To explore whether Lnc-PDZD7 could bind to miR-101 to release its inhibition of EZH2, a luciferase reporter assay was performed to test the binding of Lnc-PDZD7 and EZH2 with miR-101. RIP assays further demonstrated that Lnc-PDZD7 could directly bind to miR-101. Taken together, we demonstrated that Lnc-PDZD7 could directly



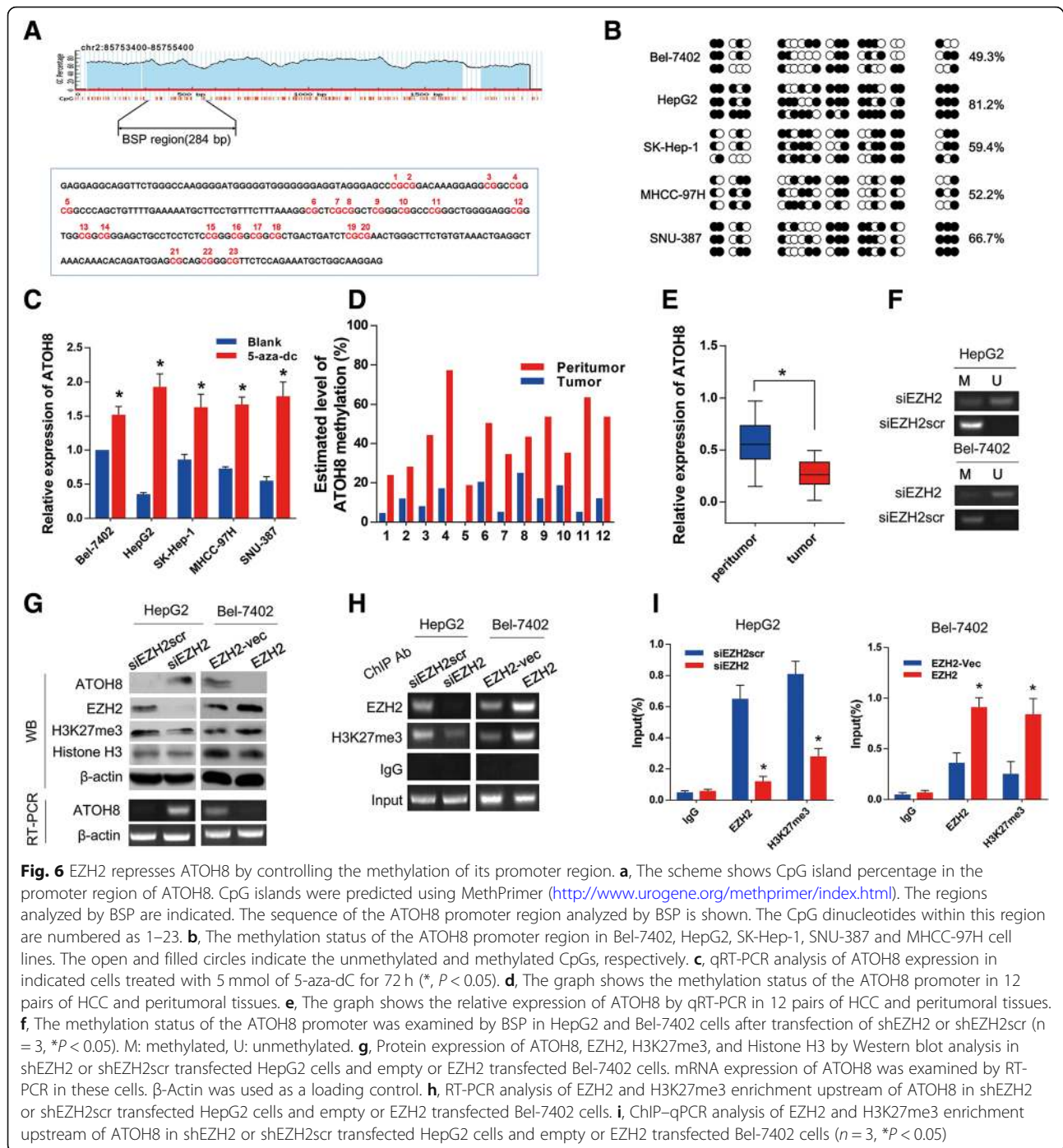


**Fig. 6** EZH2 represses ATOH8 by controlling the methylation of its promoter region. **a**, The scheme shows CpG island percentage in the promoter region of ATOH8. CpG islands were predicted using MethPrimer (<http://www.urogene.org/methprimer/index.html>). The regions analyzed by BSP are indicated. The sequence of the ATOH8 promoter region analyzed by BSP is shown. The CpG dinucleotides within this region are numbered as 1–23. **b**, The methylation status of the ATOH8 promoter region in Bel-7402, HepG2, SK-Hep-1, SNU-387 and MHCC-97H cell lines. The open and filled circles indicate the unmethylated and methylated CpGs, respectively. **c**, qRT-PCR analysis of ATOH8 expression in indicated cells treated with 5 mmol of 5-aza-dC for 72 h (\*,  $P < 0.05$ ). **d**, The graph shows the methylation status of the ATOH8 promoter in 12 pairs of HCC and peritumoral tissues. **e**, The graph shows the relative expression of ATOH8 by qRT-PCR in 12 pairs of HCC and peritumoral tissues. **f**, The methylation status of the ATOH8 promoter was examined by BSP in HepG2 and Bel-7402 cells after transfection of shEZH2 or shEZH2scr ( $n = 3$ , \* $P < 0.05$ ). M: methylated, U: unmethylated. **g**, Protein expression of ATOH8, EZH2, H3K27me3, and Histone H3 by Western blot analysis in shEZH2 or shEZH2scr transfected HepG2 cells and empty or EZH2 transfected Bel-7402 cells. mRNA expression of ATOH8 was examined by RT-PCR in these cells.  $\beta$ -Actin was used as a loading control. **h**, RT-PCR analysis of EZH2 and H3K27me3 enrichment upstream of ATOH8 in shEZH2 or shEZH2scr transfected HepG2 cells and empty or EZH2 transfected Bel-7402 cells. **i**, ChIP-qPCR analysis of EZH2 and H3K27me3 enrichment upstream of ATOH8 in shEZH2 or shEZH2scr transfected HepG2 cells and empty or EZH2 transfected Bel-7402 cells ( $n = 3$ , \* $P < 0.05$ )

interact with and downregulate miR-101 and then increase EZH2 expression.

EZH2, a histone methyltransferase, is component of the PRC2 complex. Alteration of EZH2 directly modulates the trimethylation of H3K27 and DNA methylation of CpG islands [22]. Elevated expression of EZH2 has been described in a broad range of cancer types including liver cancer [23–26]. The role of EZH2 in cancer could be linked to its activity in self-renewal promotion

and in the maintenance of the undifferentiated state of cells [27]. Studies have shown that EZH2 could directly bind to and methylate STAT3, thereby promoting the tumorigenicity of glioblastoma and prostate CSCs [8]. EZH2 can also strengthen the stem cell-like phenotype of gastric cancer via the AKT/PTEN signaling pathway [28]. However, the EZH2 regulation mechanism of the hepatic cancer stem cell phenotype is not well understood. ATOH8 belongs to a group of basic-helix-loop-helix

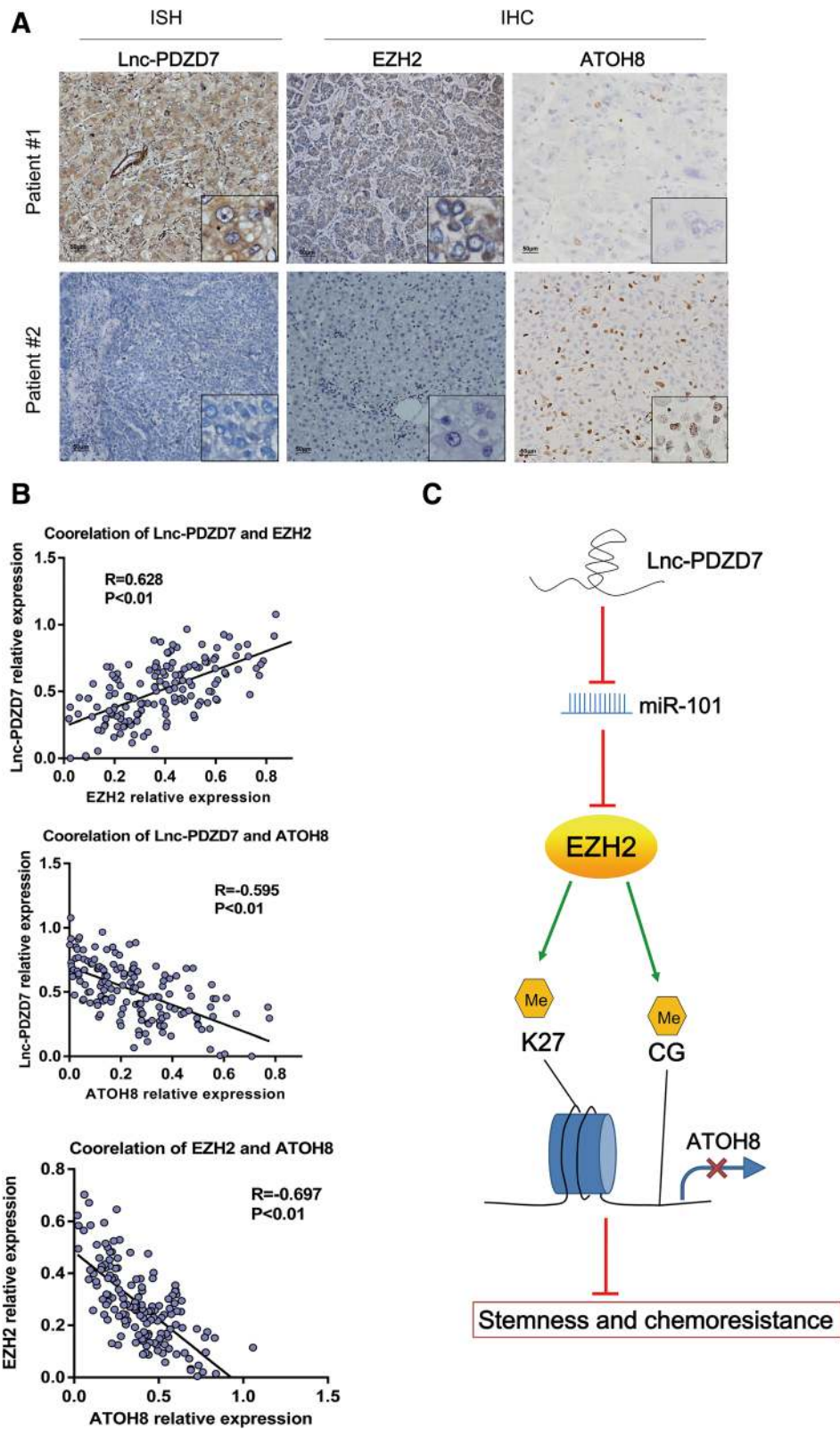


Fig. 7 (See legend on next page.)

(See figure on previous page.)

**Fig. 7** The correlation between Lnc-PDZD7, EZH2, ATOH8 and TACE response in HCC cases. **a**, Two representative cases (Patent #1 and #2) of Lnc-PDZD7, EZH2 and ATOH8 expression detected by ISH or IHC. **b**, The upper graph shows the correlation between Lnc-PDZD7 and EZH2 expression ( $r = 0.628$ ,  $P < 0.01$ ). The middle graph shows the correlation between Lnc-PDZD7 and ATOH8 expression ( $r = 0.595$ ,  $P < 0.01$ ). The lower graph shows the correlation between EZH2 and ATOH8 expression ( $r = -0.697$ ,  $P < 0.05$ ). **c**, Schematic model of the mechanism of the Lnc-PDZD7-miR-101-EZH2-ATOH8 axis in HCC

(bHLH) transcription factors and contains 321 amino acids with a bHLH domain that typically binds to a consensus sequence (CANNTG) E-box to regulate gene expression [14, 29]. Song et al. [2] discovered that ATOH8 can repress stem-cell associated genes, including OCT4, NANOG, and CD133, by contacting DNA sequences harboring an E-box motif, decreasing the stemness features and chemoresistance of HCC and suggesting that ATOH8 functions as an inhibitor of stemness features in HCC. In our research, we discovered that ATOH8 is the downstream regulator of EZH2. Then, we explored the mechanism of EZH2 regulating ATOH8 expression. We found that EZH2 could bind close to the ATOH8 promoter, EZH2 knockdown restored the ATOH8 transcript level by decreasing the DNA methylation status, and suppression of EZH2 caused an increase in ATOH8, accompanied by a reduction in the level of H3K27 methylation. These results establish a mechanism where the reduction of ATOH8 is a consequence of EZH2-mediated epigenetic silencing.

In summary, our study has identified Lnc-PDZD7 as a previously unknown negative master regulator of liver cancer stemness. In addition, we also observed that Lnc-PDZD7 can strengthen the chemosensitivity of liver cancer and is associated with prognosis and TACE response. More importantly, we demonstrate for the first time that Lnc-PDZD7 regulates stemness and chemosensitivity via EZH2 and its downstream effector ATOH8. As a downstream effector, overexpression of EZH2 can inhibit ATOH8 expression via elevating H3K27 trimethylation and DNA methylation. Therefore, our findings not only reveal the mechanism regarding Lnc-PDZD7 regulating stemness and chemosensitivity but also provide new potential therapeutic targets and valuable prognostic markers for HCC.

## Conclusions

Lnc-PDZD7 is frequently upregulated in HCC and associated with poorer prognoses and poor response to adjuvant transarterial chemoembolization therapy. Lnc-PDZD7 could promote stemness features and suppress the sensitivity of HCC cells to anticancer drugs in vitro and in vivo. Mechanistically, Lnc-PDZD7 functioned as a molecular sponge for miR-101, antagonizing its ability to repress EZH2 expression, which can further inhibit the expression of the stemness regulator ATOH8 (Fig. 7c). These findings uncover a complex regulatory mechanism of the Lnc-PDZD7/miR-101/EZH2/ATOH8 axis regulating stemness properties and chemosensitivity,

providing new biomarkers for diagnosis and potential drug targets for HCC.

## Additional files

**Additional file 1: Figure S1.** Heatmap representation of 26 upregulated lncRNAs in HCC tissues compared to para-tumorous tissues ( $P < 0.01$  and fold change  $> 6$ ). (TIF 2527 kb)

**Additional file 2: Table S1.** Multivariate survival analysis of five-year overall and relapse-free survival in 152 HCC patients (DOC 44 kb)

**Additional file 3: Figure S2.** Lnc-PDZD7 increase the CSC markers in HCC cells. Expression of CD133, OCT4, NANOG, SOX2 were examined by qRT-PCR in siLnc-scr and siLnc-PDZD7 transfected HepG2 cells and Lnc-PDZD7 and Lnc-vec transfected Bel-7402 cells ( $*P < 0.05$ ). (TIF 1203 kb)

**Additional file 4: Figure S3** EZH2 is a functional downstream target of miR-101. **A**, Lnc-PDZD7 was precipitated using a Lnc-PDZD7 specific probe or control probe. Lnc-PDZD7 and miR-101 were detected in the precipitates using qRT-PCR in HepG2 and Bel-7402 cells. **B**, The predicted sites of miR-101 binding to the 3'-UTR region of EZH2 were detected using bioinformatics prediction tools. The mutated site in the 3'-UTR region of EZH2 is shown (EZH2 3'-UTR mut-1 and mut-2). **C**, The effect of miR-101 on the luciferase activity induced by the EZH2 3'-UTR wt, EZH2 3'-UTR mut-1 and 3'-UTR mut-2 reporter plasmids was measured by luciferase reporter gene assay in HepG2 and Bel-7402 cells ( $*P < 0.05$ ). (TIF 2333 kb)

**Additional file 5: Figure S4.** EZH2 is a functional downstream target of Lnc-PDZD7 in HCC cells. **A**, The mRNA level of EZH2, CD133, OCT4, NANOG and SOX2 were examined by qRT-PCR in EZH2 plasmid or EZH2-vec transfected Lnc-PDZD7-depleted HepG2 cells. **B**, Sphere formation in EZH2 plasmid or EZH2-vec transfected Lnc-PDZD7-depleted HepG2 cells. **C**, Cell viability was examined by MTT assay. The cell viability under different concentrations of 5-Fu treatment in EZH2 plasmid or EZH2-vec transfected Lnc-PDZD7-depleted HepG2 cells. **E**, The mRNA level of EZH2, CD133, OCT4, NANOG and SOX2 were examined by qRT-PCR in shEZH2 or shEZH2scr transfected Lnc-PDZD7-overexpressing Bel-7402 cells. **F**, Sphere formation in siEZH2 or siEZH2scr transfected Lnc-PDZD7-overexpressing Bel-7402 cells. **G**, The cell viability under different concentrations of sorafenib treatment in siEZH2 or siEZH2scr transfected Lnc-PDZD7-overexpressing Bel-7402 cells. The data are shown as the means  $\pm$  S.D. of three replicates ( $*P < 0.05$ ). (TIF 1847 kb)

**Additional file 6: Figure S5.** Lnc-PDZD7 negatively regulate ATOH8 expression in HCC spheres. Expression of ATOH8 were examined by qRT-PCR in siLnc-scr and siLnc-PDZD7 transfected HepG2 spheres and Lnc-PDZD7 and Lnc-vec transfected Bel-7402 spheres ( $*P < 0.05$ ). (TIF 1061 kb)

## Abbreviations

BSP: Bisulfite genomic sequencing; ChIP: Chromatin immunoprecipitation; CSC: Cancer stem cell; HCC: Hepatocellular carcinoma; IHC: Immunohistochemistry; ISH: In situ hybridization; lncRNA: Long noncoding RNA; MSP: Methylation-specific PCR; OS: Overall survival; qRT-PCR: Quantitative real time RT-PCR; TACE: Transcatheter arterial chemoembolization

## Acknowledgements

Not applicable.

### Funding

This research was supported in part by the National Natural Science Foundation of China (No. 81702435, No. 81430014, No. 81360367, No. 81560393), the Natural Science Foundation of Guangxi (2015GXNSFDA139026), the Natural Science Foundation of Jiangsu (BK20170264), the China Postdoctoral Science Foundation (2018 M630606), the Guangxi Science Fund for Distinguished Young Scholars Program (2016GXNSFFA380003), the 111 Project (D17011), Bagui Scholars Guangxi, the Natural Science Foundation of Guangxi (2016GXNSFBA380043), the Project of Scientific Research and Technological Development of Guilin (2016012706–14) and 2017 Guilin Talents Heights Construction Funding Project.

### Availability of data and materials

The datasets used and/or analysed during the current study are available from the corresponding author on reasonable request.

### Authors' contributions

YZ, BT and SQH developed the original hypothesis and supervised the experimental design; YZ, BT and SPY performed in vitro and in vivo experiments; YZ, YL and HZS participated in the clinical specimens detection; YL, HZS and JS analyzed data and performed statistical analysis; YZ, BT and SQH wrote and revise the manuscript. All authors read and approved the final manuscript.

### Ethics approval and consent to participate

All participants provided written informed consent, and the study was approved by the ethics committee of The Affiliated Hospital of Guangxi Medical University. All animal experiments complied with the Policy of Guangxi Medical University on the Care and Use of Laboratory Animals.

### Consent for publication

Not applicable.

### Competing interests

The authors declare that they have no competing interests.

### Publisher's Note

Springer Nature remains neutral with regard to jurisdictional claims in published maps and institutional affiliations.

### Author details

<sup>1</sup>Department of Hepatobiliary Surgery, The First Affiliated Hospital of Guangxi Medical University, No.6 Shuangyong Road, Nanning, Guangxi 530021, People's Republic of China. <sup>2</sup>Department of General Surgery, Affiliated hospital of Xuzhou Medical University, Xuzhou 221000, China.

Received: 2 November 2018 Accepted: 13 February 2019

Published online: 20 February 2019

### References

- Gores GJ. Decade in review-hepatocellular carcinoma: HCC-subtypes, stratification and sorafenib. *Nat Rev Gastroenterol Hepatol*. 2014;11:645–7.
- Song Y, Pan G, Chen L, Ma S, Zeng T, Man Chan TH, et al. Loss of ATOH8 increases stem cell features of hepatocellular carcinoma cells. *Gastroenterology*. 2015;149:1068–81.
- Yuan SX, Wang J, Yang F, Tao QF, Zhang J, Wang LL, et al. Long noncoding RNA DANCR increases stemness features of hepatocellular carcinoma by derepression of CTNNB1. *Hepatology*. 2016;63:499–511.
- Necsulea A, Soumillon M, Warnefors M, Liechti A, Daish T, Zeller U, et al. The evolution of lncRNA repertoires and expression patterns in tetrapods. *Nature*. 2014;505:635–40.
- Mercer TR, Dinger ME, Mattick JS. Long non-coding RNAs: insights into functions. *Nat Rev Genet*. 2009;10:155–9.
- Fu Z, Chen C, Zhou Q, Wang Y, Zhao Y, Zhao X, et al. LncRNA HOTTIP modulates cancer stem cell properties in human pancreatic cancer by regulating HOXA9. *Cancer Lett*. 2017;410:68–81.
- Chen H, Ren C, Han C, Wang D, Chen Y, Fu D. Expression and prognostic value of miR-486-5p in patients with gastric adenocarcinoma. *PLoS One*. 2015;10:e0119384.
- Kim E, Kim M, Woo DH, Shin Y, Shin J, Chang N, et al. Phosphorylation of EZH2 activates STAT3 signaling via STAT3 methylation and promotes Tumorigenicity of glioblastoma stem-like cells. *Cancer Cell*. 2013;23:839–52.
- Chang C, Yang J, Xia W, Chen C, Xie X, Chao C, et al. EZH2 promotes expansion of breast tumor initiating cells through activation of RAF1- $\beta$ -catenin signaling. *Cancer Cell*. 2011;19:86–100.
- Gonzalez M, Moore H, Li X, Toy K, Huang W, Sabel M, et al. EZH2 expands breast stem cells through activation of NOTCH1 signaling. *Proc Natl Acad Sci U S A*. 2014;111:3098–103.
- Tay Y, Rinn J, Pandolfi PP. The multilayered complexity of ceRNA crosstalk and competition. *Nature*. 2014;505:344–52.
- Xu L, Beckebaum S, Iacob S, Wu G, Kaiser GM, Radtke A, et al. MicroRNA-101 inhibits human hepatocellular carcinoma progression through EZH2 downregulation and increased cytostatic drug sensitivity. *J Hepatol*. 2014;60:590–8.
- Zheng F, Liao Y, Cai M, Liu T, Chen S, Wu P, et al. Systemic delivery of microRNA-101 potently inhibits hepatocellular carcinoma in vivo by repressing multiple targets. *PLoS Genet*. 2015;11:e1004873.
- Ejarque M, Altirriba J, Gomis R, Gasa R. Characterization of the transcriptional activity of the basic helix-loop-helix (bHLH) transcription factor Atoh8. *Biochim Biophys Acta*. 2013;1829:1175–83.
- Cedar H, Bergman Y. Linking DNA methylation and histone modification: patterns and paradigms. *Nat Rev Genet*. 2009;10:295–304.
- Lo Re O, Fusilli C, Rappa F, Van Haele M, Douet J, Pindjakova J, et al. Induction of cancer cell stemness by depletion of macrohistone H2A1 in hepatocellular carcinoma. *Hepatology*. 2018;67:636–50.
- Chen HA, Kuo TC, Tseng CF, Ma JT, Yang ST, Yen CJ, et al. Angiopoietin-like protein 1 antagonizes MET receptor activity to repress sorafenib resistance and cancer stemness in hepatocellular carcinoma. *Hepatology*. 2016;64:1637–51.
- O'Connor ML, Xiang D, Shigdar S, Macdonald J, Li Y, Wang T, et al. Cancer stem cells: a contentious hypothesis now moving forward. *Cancer Lett*. 2014;344:180–7.
- Wu J, Crowe DL. The histone methyltransferase EZH2 promotes mammary stem and luminal progenitor cell expansion, metastasis and inhibits estrogen receptor-positive cellular differentiation in a model of basal breast cancer. *Oncol Rep*. 2015;34:455–60.
- Suva ML, Riggi N, Janiszewska M, Radovanovic I, Provero P, Stehle JC, et al. EZH2 is essential for glioblastoma cancer stem cell maintenance. *Cancer Res*. 2009;69:9211–8.
- Jin X, Kim LJY, Wu Q, Wallace LC, Prager BC, Sanvoranart T, et al. Targeting glioma stem cells through combined BMI1 and EZH2 inhibition. *Nat Med*. 2017;23:1352–61.
- Vire E, Brenner C, Deplus R, Blanchon L, Fraga M, Didelot C, et al. The Polycomb group protein EZH2 directly controls DNA methylation. *Nature*. 2006;439:871–4.
- Varambally S, Dhanasekaran SM, Zhou M, Barrette TR, Kumar-Sinha C, Sanda MG, et al. The polycomb group protein EZH2 is involved in progression of prostate cancer. *Nature*. 2002;419:624–9.
- Matsukawa Y, Semba S, Kato H, Ito A, Yanagihara K, Yokozaki H. Expression of the enhancer of zeste homolog 2 is correlated with poor prognosis in human gastric cancer. *Cancer Sci*. 2006;97:484–91.
- Kleer CG, Cao Q, Varambally S, Shen R, Ota I, Tomlins SA, et al. EZH2 is a marker of aggressive breast cancer and promotes neoplastic transformation of breast epithelial cells. *Proc Natl Acad Sci U S A*. 2003;100:11606–11.
- Sudo T, Utsunomiya T, Mimori K, Nagahara H, Ogawa K, Inoue H, et al. Clinicopathological significance of EZH2 mRNA expression in patients with hepatocellular carcinoma. *Br J Cancer*. 2005;92:1754–8.
- Marchesi I, Bagella L. Targeting enhancer of Zeste homolog 2 as a promising strategy for cancer treatment. *World journal of clinical oncology*. 2016;7:135–48.
- Gan L, Xu M, Hua R, Tan C, Zhang J, Gong Y, et al. The polycomb group protein EZH2 induces epithelial-mesenchymal transition and pluripotent phenotype of gastric cancer cells by binding to PTEN promoter. *J Hematol Oncol*. 2018;11:9.
- Patel N, Varghese J, Masaratana P, Latunde-Dada GO, Jacob M, Simpson RJ, et al. The transcription factor ATOH8 is regulated by erythropoietic activity and regulates HAMP transcription and cellular pSMAD1,5,8 levels. *Br J Haematol*. 2014;164:586–96.